Contact: matteo.scarponi@unil.ch
Research Group: https://www.unil.ch/orog3ny/
[1]University of Lausanne, Switzerland
[2]Czech Academy of Sciences, Prague [3]INGV, Italy

EGU General Assembly 2021

Joint receiver function and gravity inversion for new constraints on the Ivrea body structure:

2D high-resolution view along the Val Sesia profile (N. Italy)

M Scarponi[1], G Hetényi[1], J Plomerová[2], S Solarino[3]

Joint seismic and gravity inversion:
+ New **seismic Receiver Functions** (*IvreaArray* data);
+ **Gravity anomaly** from Scarponi et al. (2020 GJI);
> **2D IGB model** along the Val Sesia cross-section.

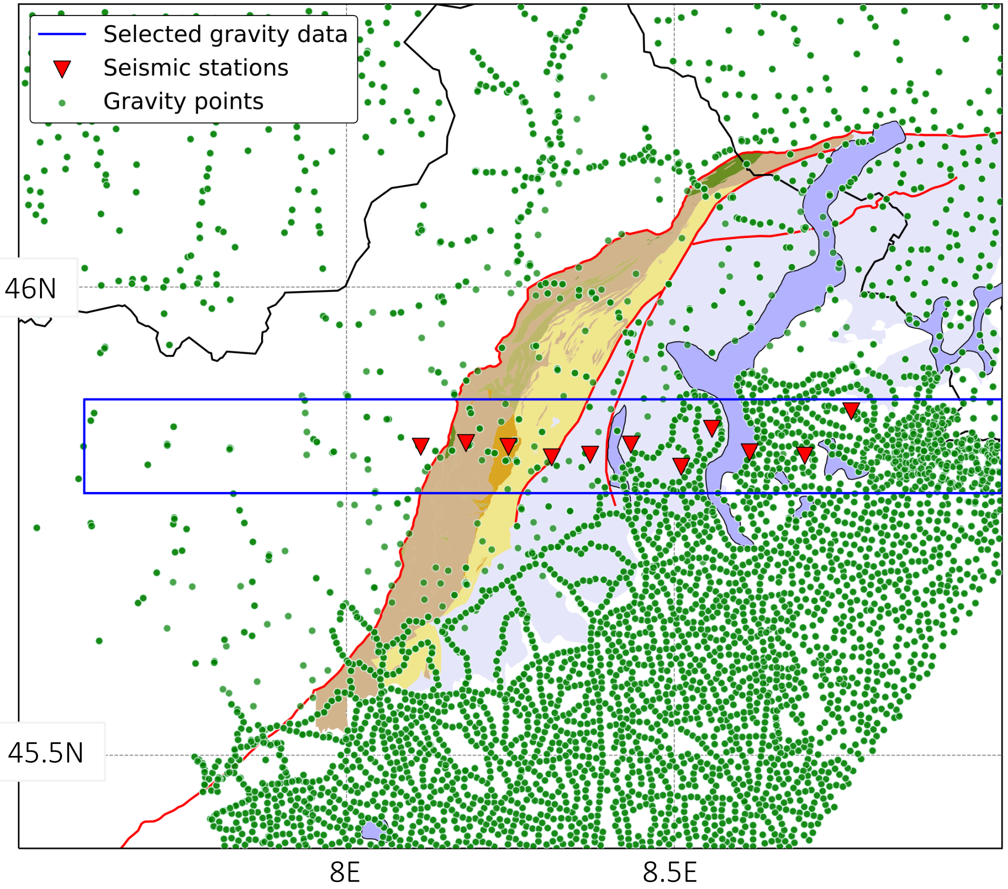

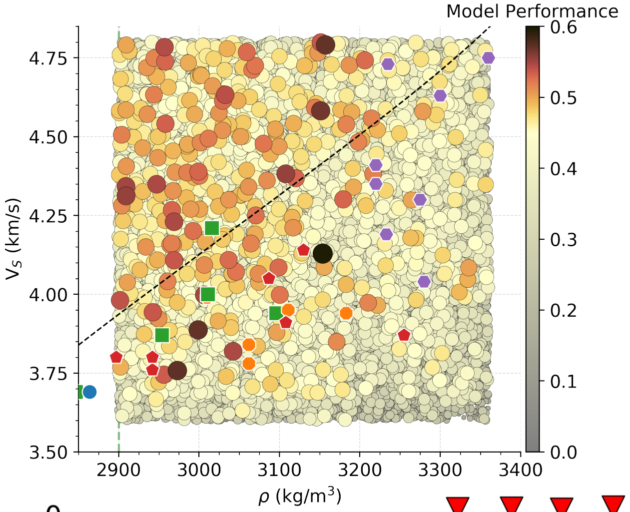

Iterative **joint inversion** algorithm:
+ Guided model space exploration
+ **RF migration & gr. anomaly** modelling
> Constrains on IGB geometry, Δv_S, $\Delta\rho$

Results currently in press:
Scarponi et al. (2021) Front. Earth Sci.

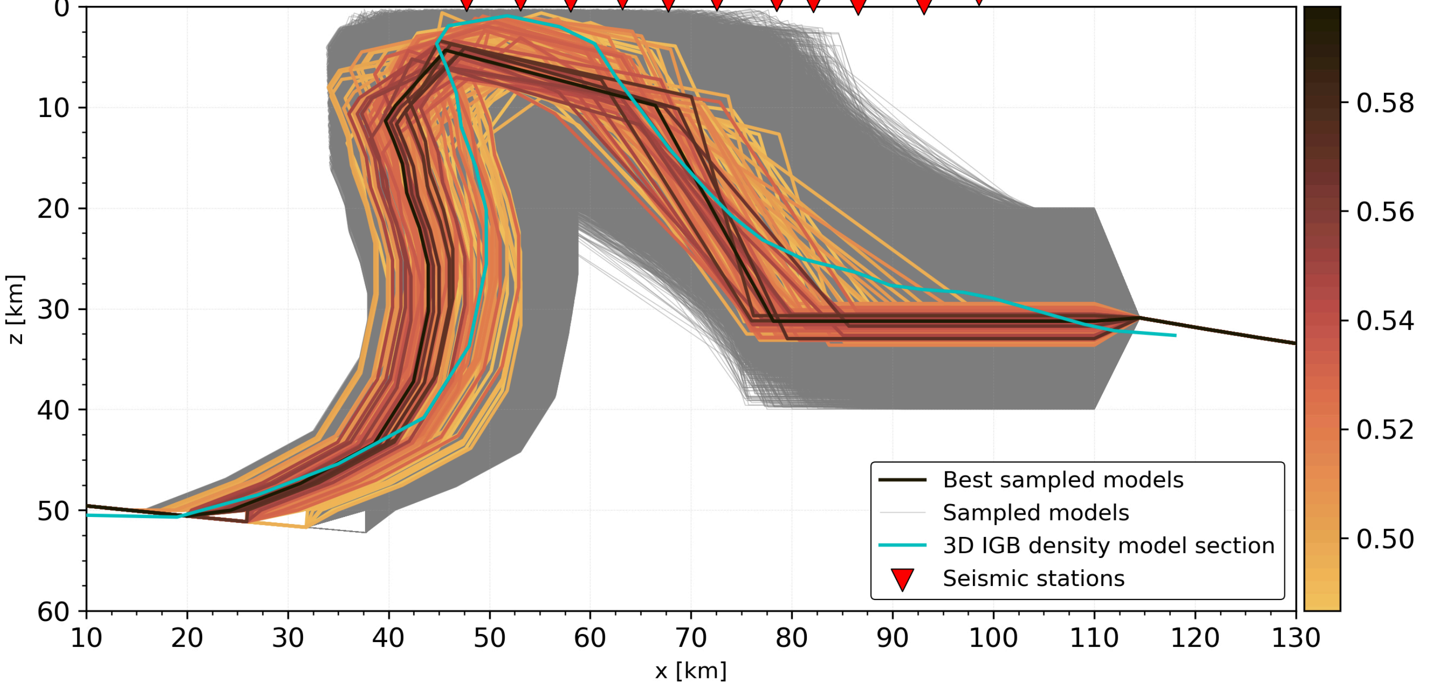

Contact: matteo.scarponi@unil.ch
Research Group: https://www.unil.ch/orog3ny/
EGU2021 26.04.2021

Joint receiver function and gravity inversion for new constraints on the Ivrea body structure:

2D high-resolution view along the Val Sesia profile (N. Italy)

M Scarponi[1], G Hetényi[1], J Plomerová[2], S Solarino[3]

Thank you for your interest in this presentation. Comment boxes will provide information to the reader. The results presented here are further discussed in:

Scarponi et al. 2021, Frontiers in Earth Sciences (In press)

[1]University of Lausanne, Switzerland
[2]Czech Academy of Sciences, Prague
[3]INGV, Italy

Study area and the Ivrea Geophysical Body (IGB)

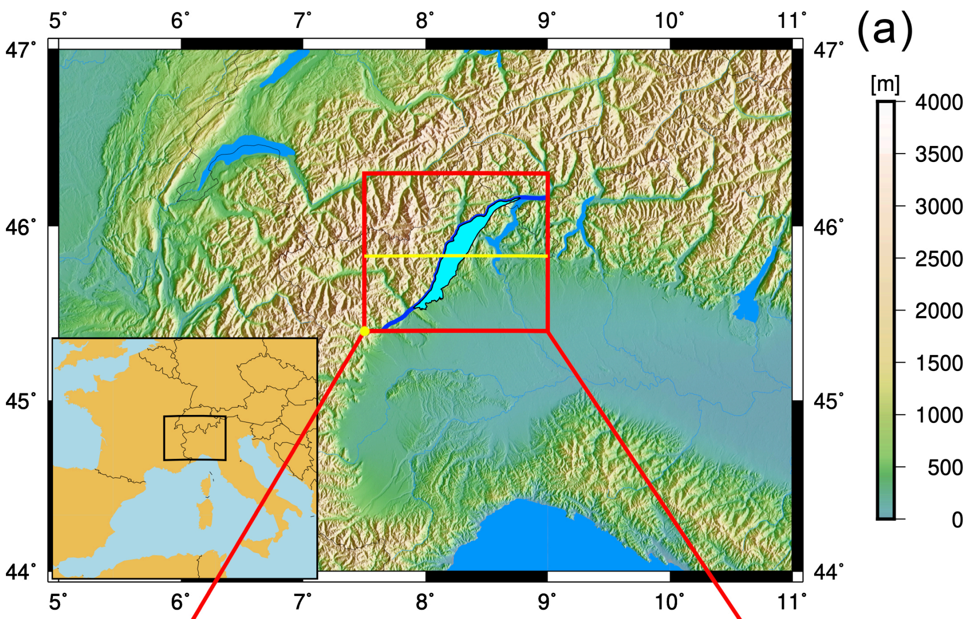

a) Study area (red box) and the 2D cross-section investigated in this study (yellow line), along the 2D West-East IvreaArray seismic profile (red triangles). The target profile extends across the IVZ (cyan shape), delimited to the West by the Insubric Line (blue line).

The yellow circle is the origin of the km-coordinate system used in this study and in the subsequent figures (7.5°E,45.4°N).

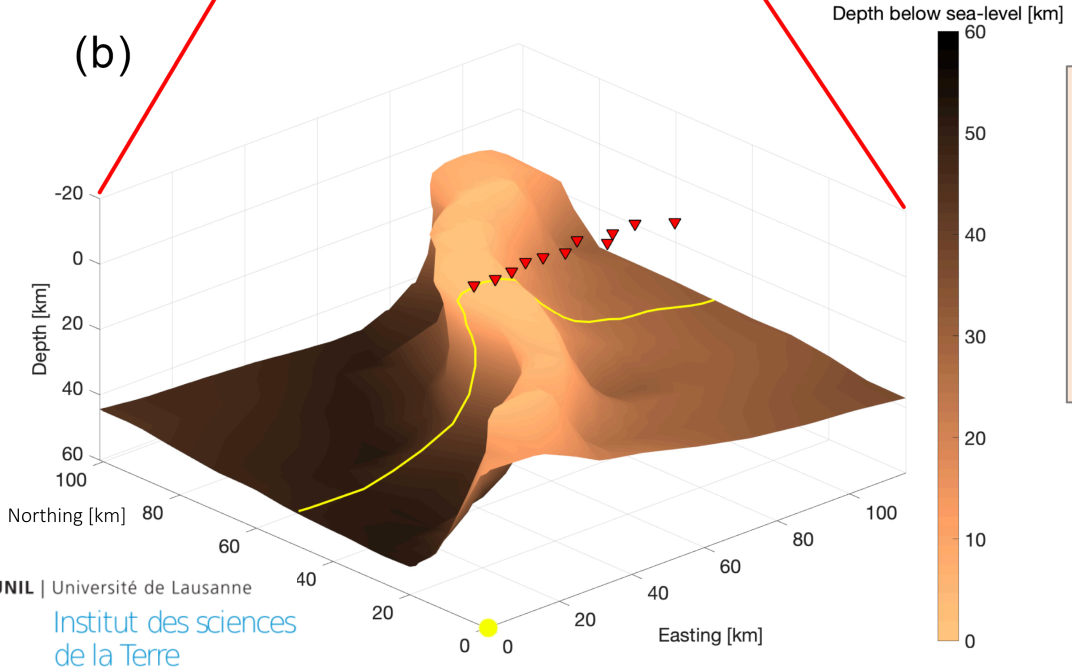

b) Perspective view of the IGB 3D density model interface constrained by gravity data modelling in an earlier study (Scarponi et al., 2020).

In this study, we aim at refining a 2D West-East cross-section of the model (yellow line), by jointly inverting the gravity data with the new seismic data we collected (IvreaArray, red triangles).

Study area geological map and data

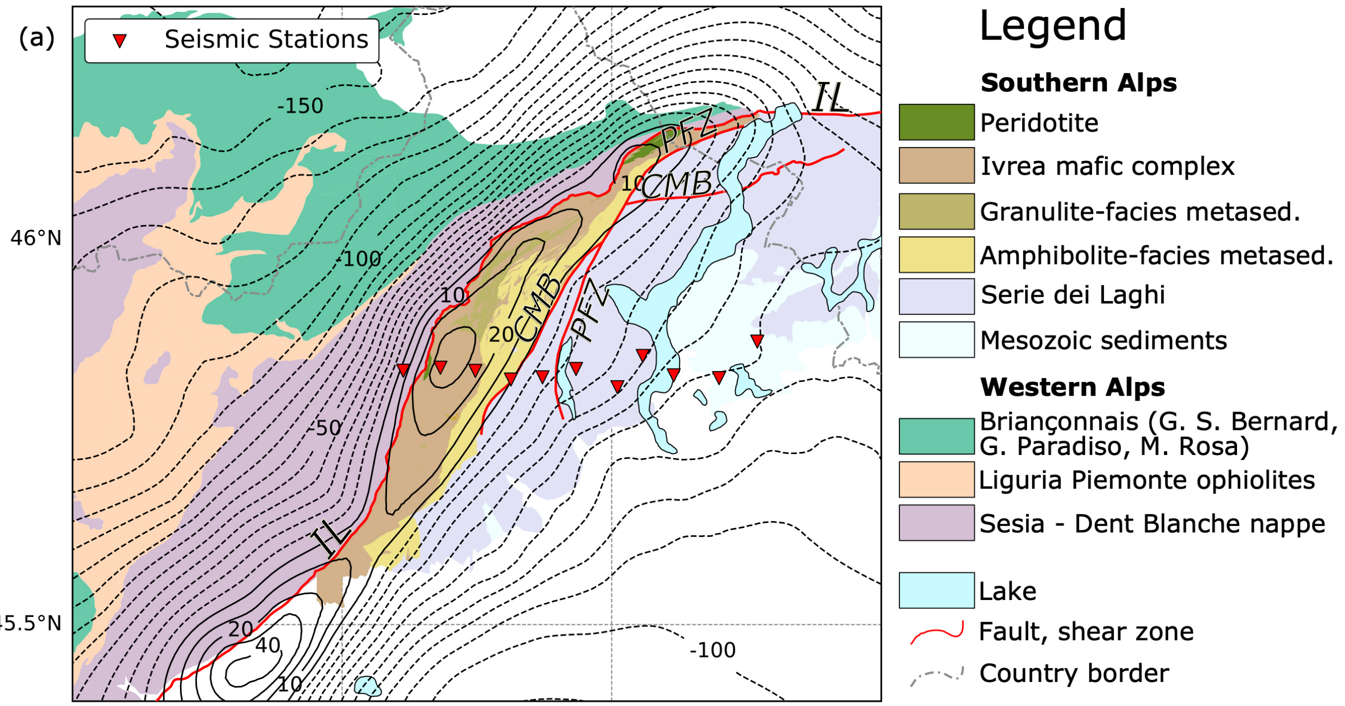

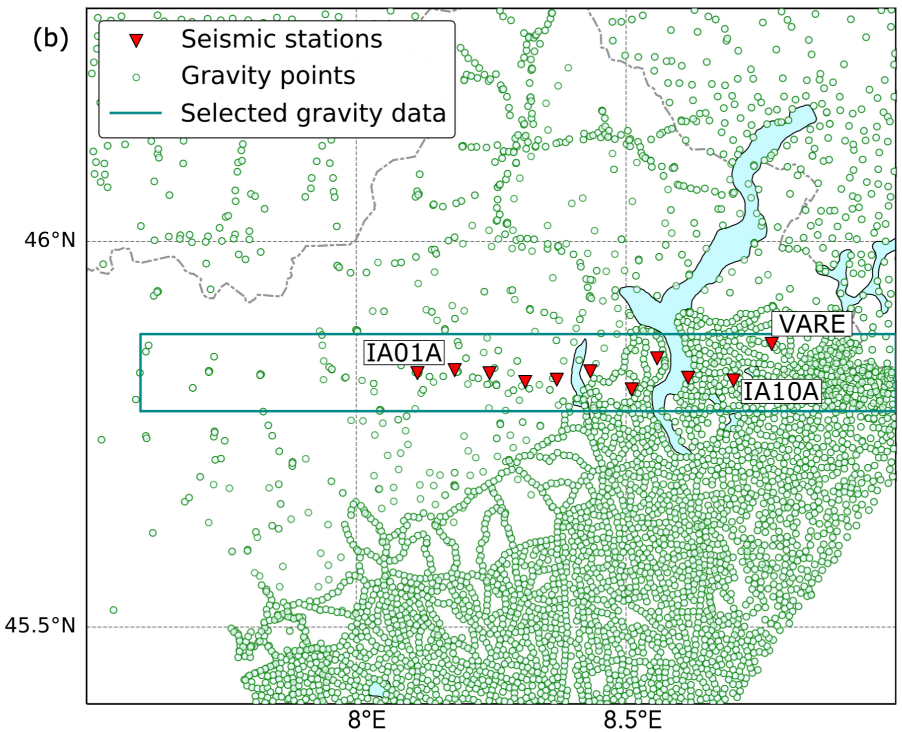

(a) Geological map of the IVZ and the surrounding areas, simplified from Petri et al. (2019) and Schmid et al. (2004). The main faults (red lines), relevant for this study, are indicated as "IL" for Insubric Line, "PFZ" for Pogallo Fault Zone and "CMB" for Cossato-Mergozzo-Brissago Line. Overlaid, the 10 mGal contour lines for the Bouguer gravity anomaly from our data across the study area.

(b) Compiled and recently collected gravity data, previously merged and processed in the scope of the work of Scarponi et al. (2020).
The cyan box indicates the gravity data we selected for this study along the 2D IvreaArray seismic profile (red triangles). The INGV permanent seismic station IV.VARE has been included in the study. IvreaArray recorded continuous seismic data for two years and three months (June 2017-September 2019).

IvreaArray seismic network: https://doi.org/10.5281/zenodo.1038209

Gravity anomaly and seismic RFs migration example

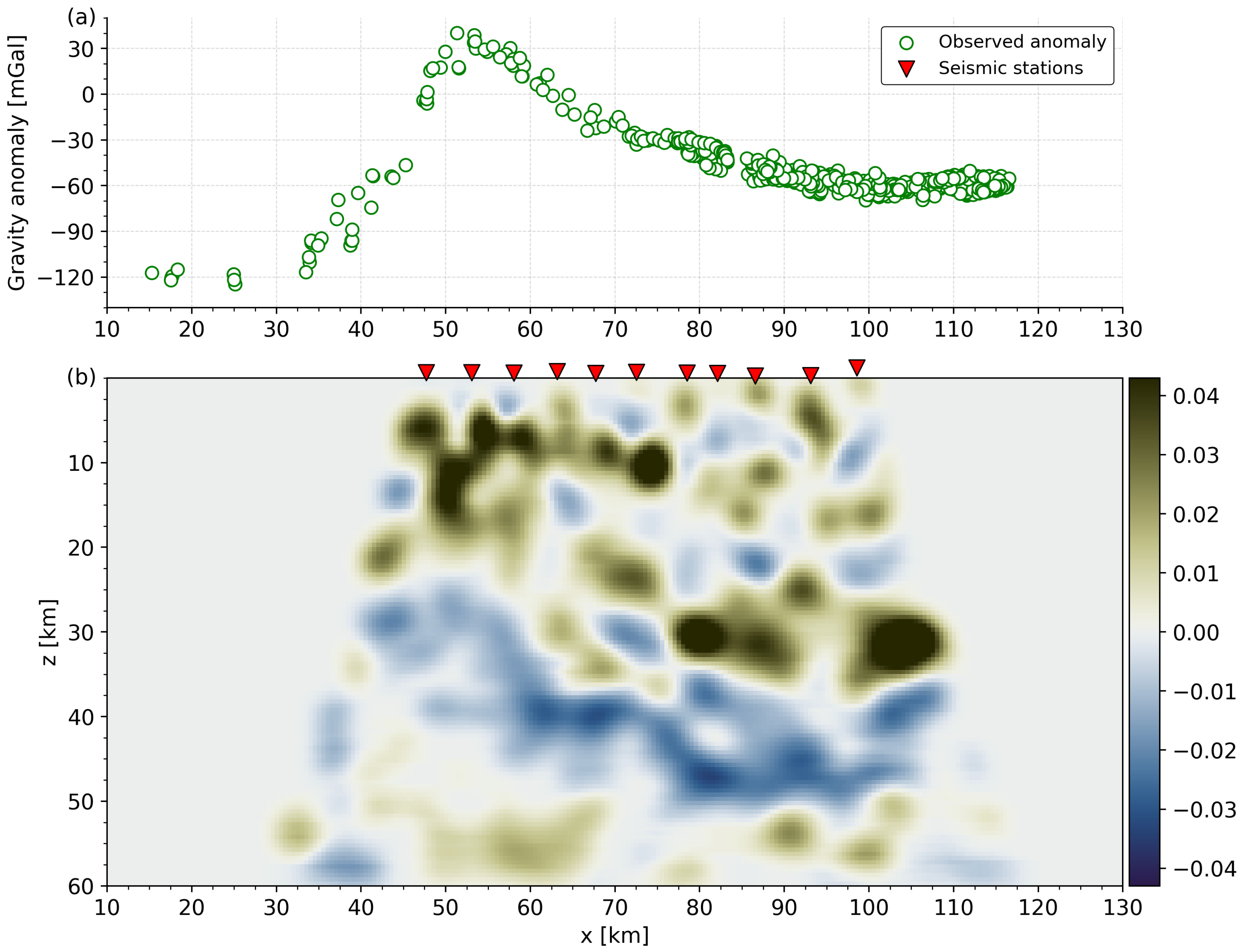

(a) Niggli gravity anomaly computed from observed data and applying rock-density-based terrain corrections (Scarponi et al. 2020) along the West-East IvreaArray profile.

(b) An example of migrated receiver function profile with the use of the IvreaArray and VARE seismic data and the iasp91 velocity model for ray-tracing and migration. Colors highlight areas of increasing (brown) and decreasing (blue) seismic velocities with depth.

Inversion workflow

Joint seismic-gravity inversion workflow, implementing a performance-driven pseudo-random walk in the model space and a performance-based selection rule for the new candidate models. Red boxes relate to the new candidate model generation and evaluation, blue boxes to the forward modelling and green boxes to the model performance evaluation.

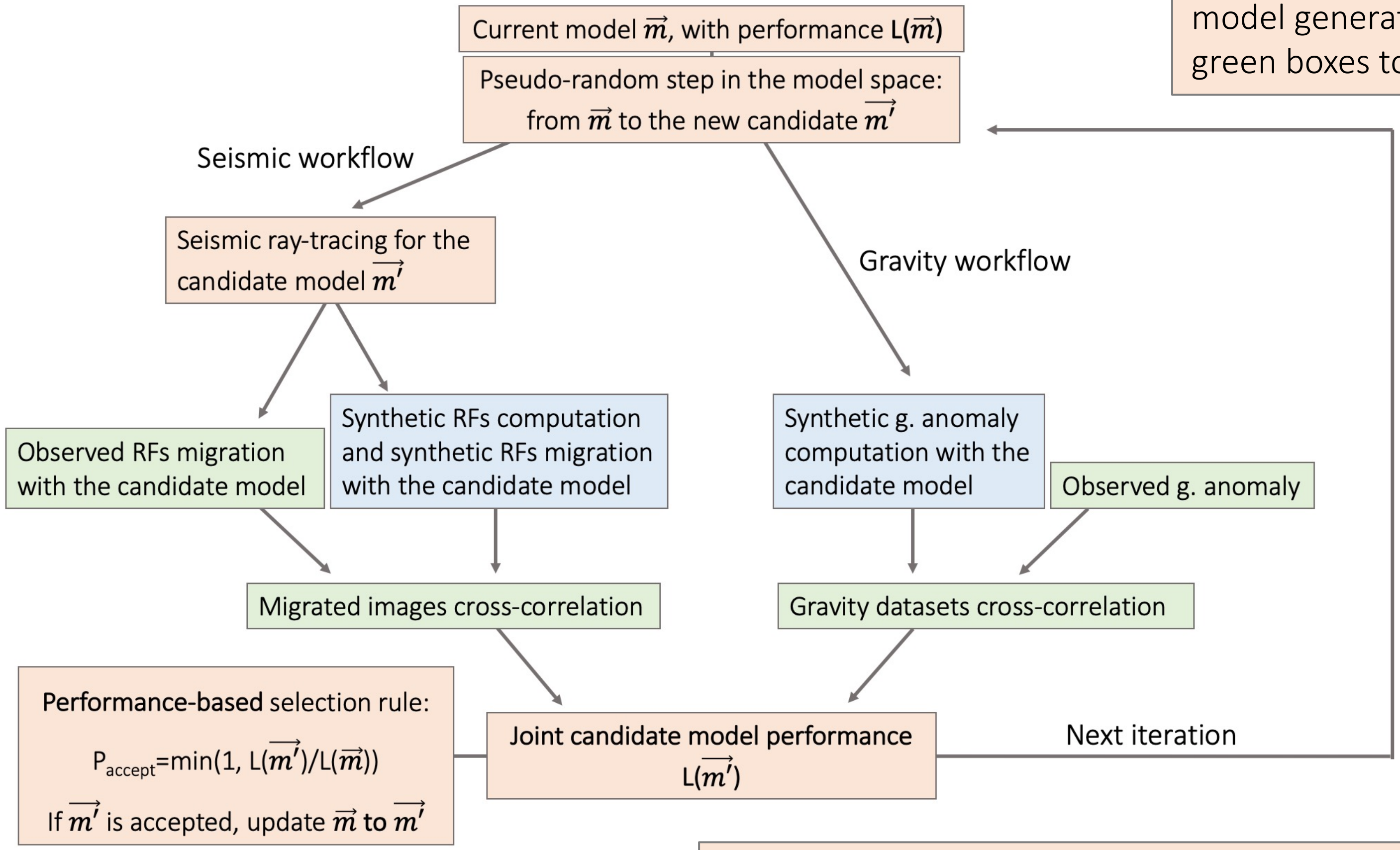

A new candidate model is proposed at each iteration, and associated with a joint seismic and gravity model performance. Based on this, the candidate is either accepted or rejected (following the idea of the Metropolis-Hastings selection rule).
The same model is used both for observed RFs migration and for generating and migrating the synthetic RFs at each iteration.

Model parameterization

IGB model parameterization for the joint seismic and gravity inversion. We invert for the 2D IGB interface geometry (black line), which is defined by four nodes. The node locations can vary within a given perimeter, together with the velocity and density contrasts associated to the IGB interface.

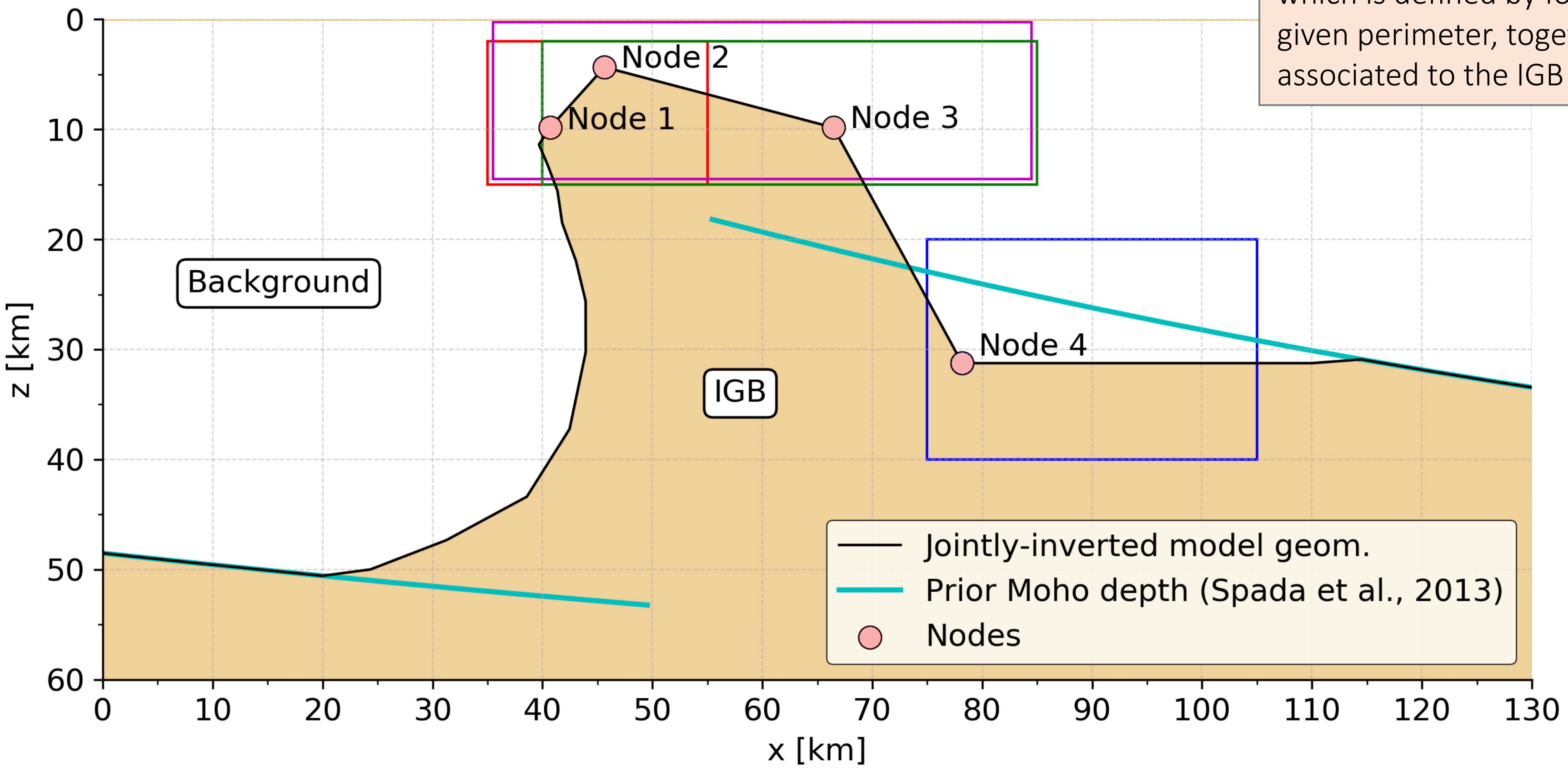

The far-field model geometry connects to the Moho map (Spada et al., 2013). In the East, the connection is by a horizontal line. In the West, the curved shape is taken from the earlier 3D gravity model of (Scarponi et al., 2020), as the vertical wall cannot be resolved by converted seismic waves.

Forward modelling (example for the best model)

(a) Model geometry, defined by four nodes.

(b) Seismic ray-tracing across the model interface for the associated velocity model. Seismic rays are colored according to the interface segment they cross along their path. The wave mode conversion respects Snell's law considering the local interface dip.

(c) Comparison between observed and synthetic gravity anomalies for the current model, and their misfit.

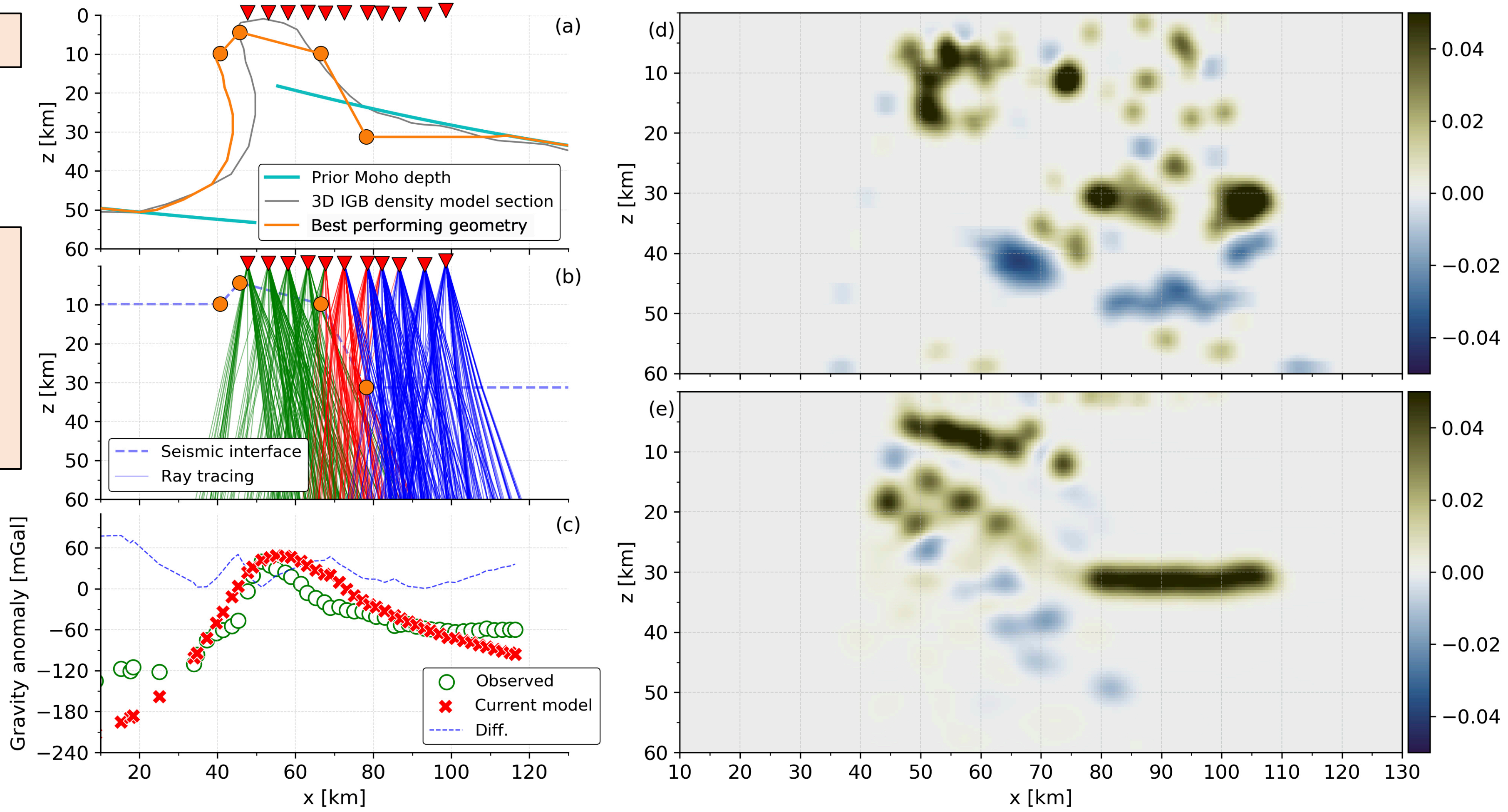

(d) Observed-RFs migration, including ray-tracing and migration with the velocity structure of the given model. (e) Synthetic-RFs migration, using RFs generated by the current velocity structure, and then treated the same way as the observed RFs. The comparison between Observed-RFs and Synthetic-RFs migrations is obtained via zero-shift image cross-correlation.

Sampled model geometries

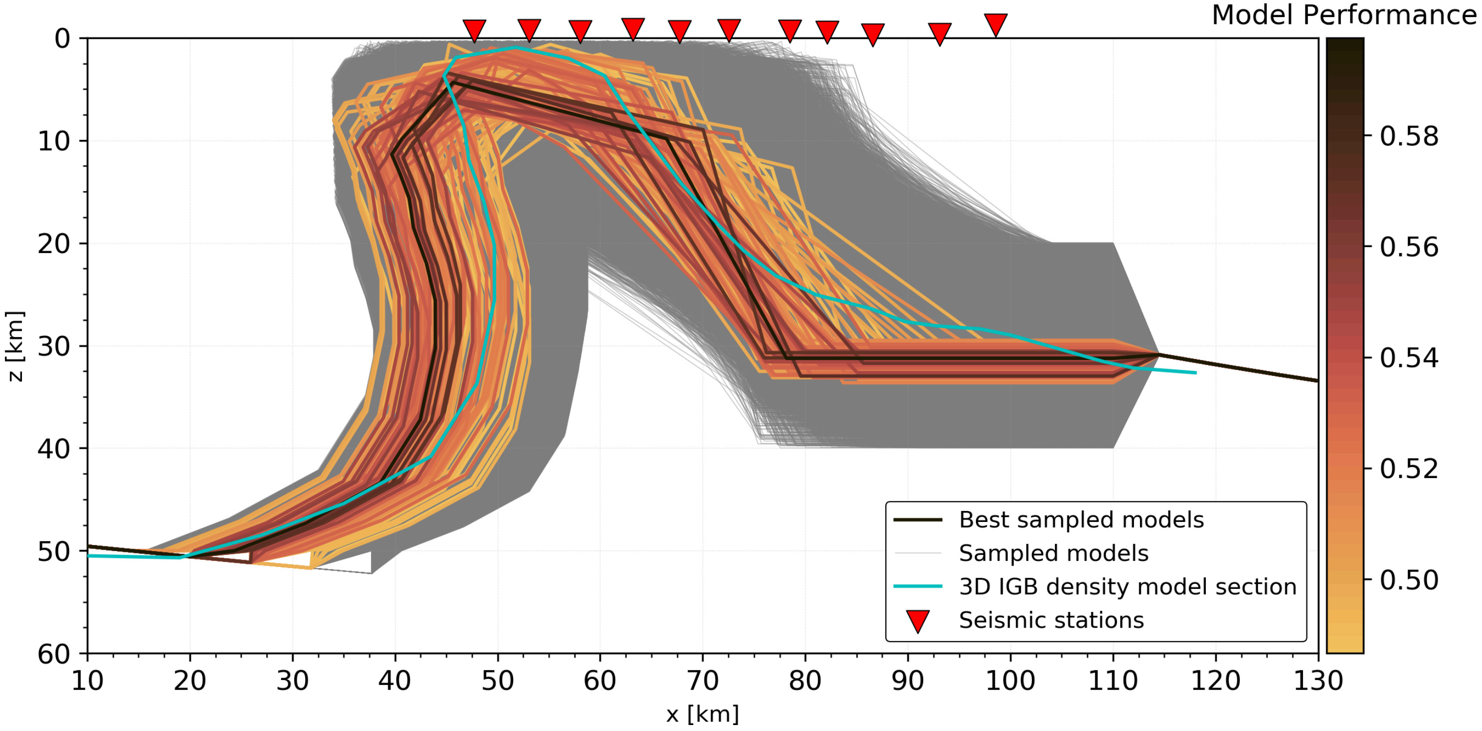

Model geometries resulting from the joint inversion. The 150 best performing models are shown in coloured lines according to the model performance. All other sampled and kept models are shown in grey (in total 41'365 models). The cyan dashed line is the cross-section through the 3D IGB gravity model from previous study (Scarponi et al. 2020).

Sampled model geometries (node by node)

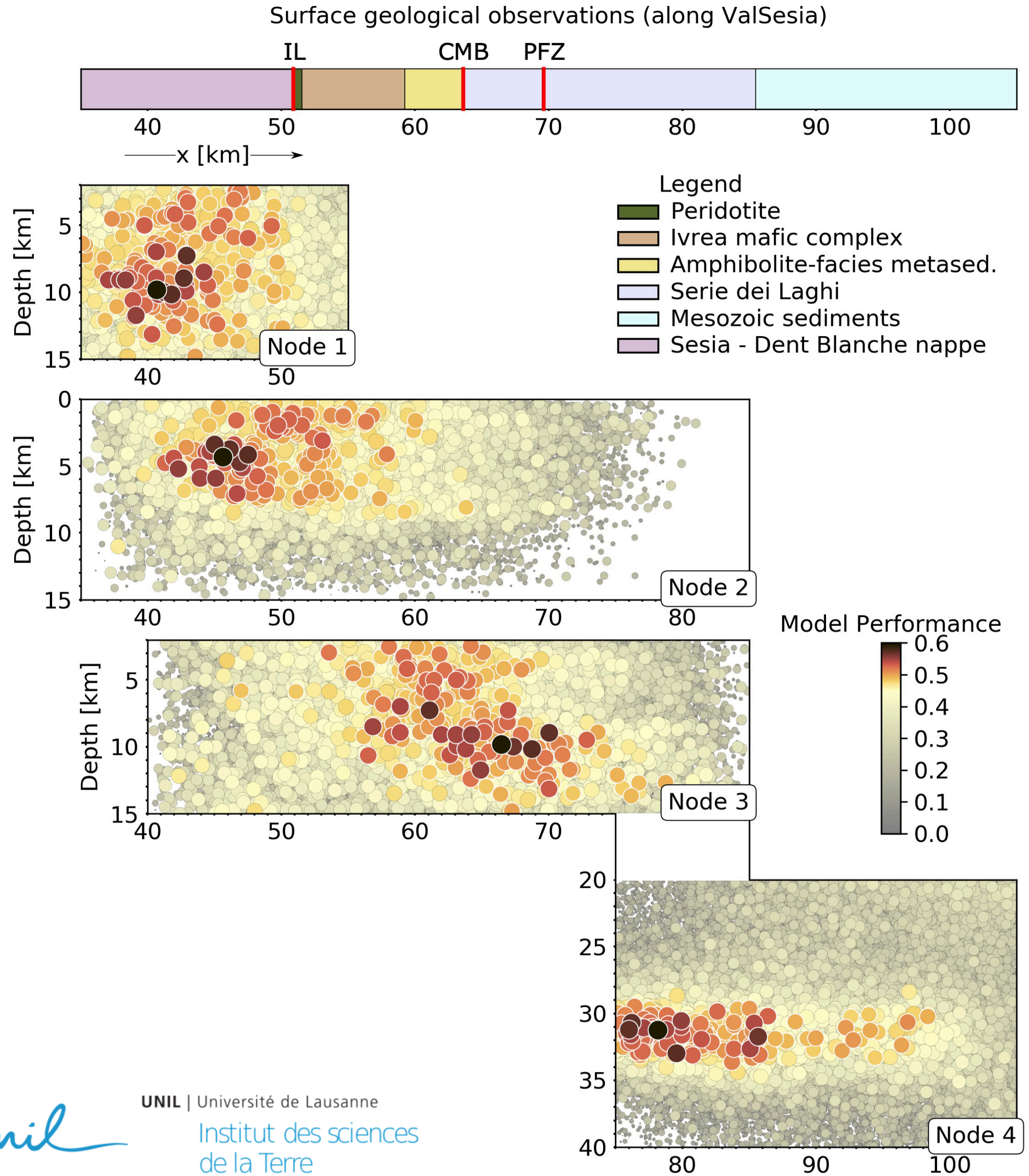

Inversion results on the position of the four nodes, presented in four distance–depth panels. Each panel is showing the locations visited by each single node during the inversion, for each sampled model. All four panels share the same horizontal x-axis, but they are shifted along the vertical direction for better visual distinction. Panels of nodes 3 and 4 share the same depth axis, too.

All sampled and kept models are shown (in total 41’363), with size and colour according to the model performance (white edges for performances > 0.48). On top, the corresponding surface geological observations from earlier studies (along the same x-axis), identifying rock types along the profile (legend on the top right, same as in Figure 2). The relevant faults for this study are indicated (as in Figure 2) as “IL” for Insubric Line, “CMB” for Cossato-Mergozzo-Brissago Line and “PFZ” for Pogallo Fault Zone.

Sampled model velocity and density contrasts

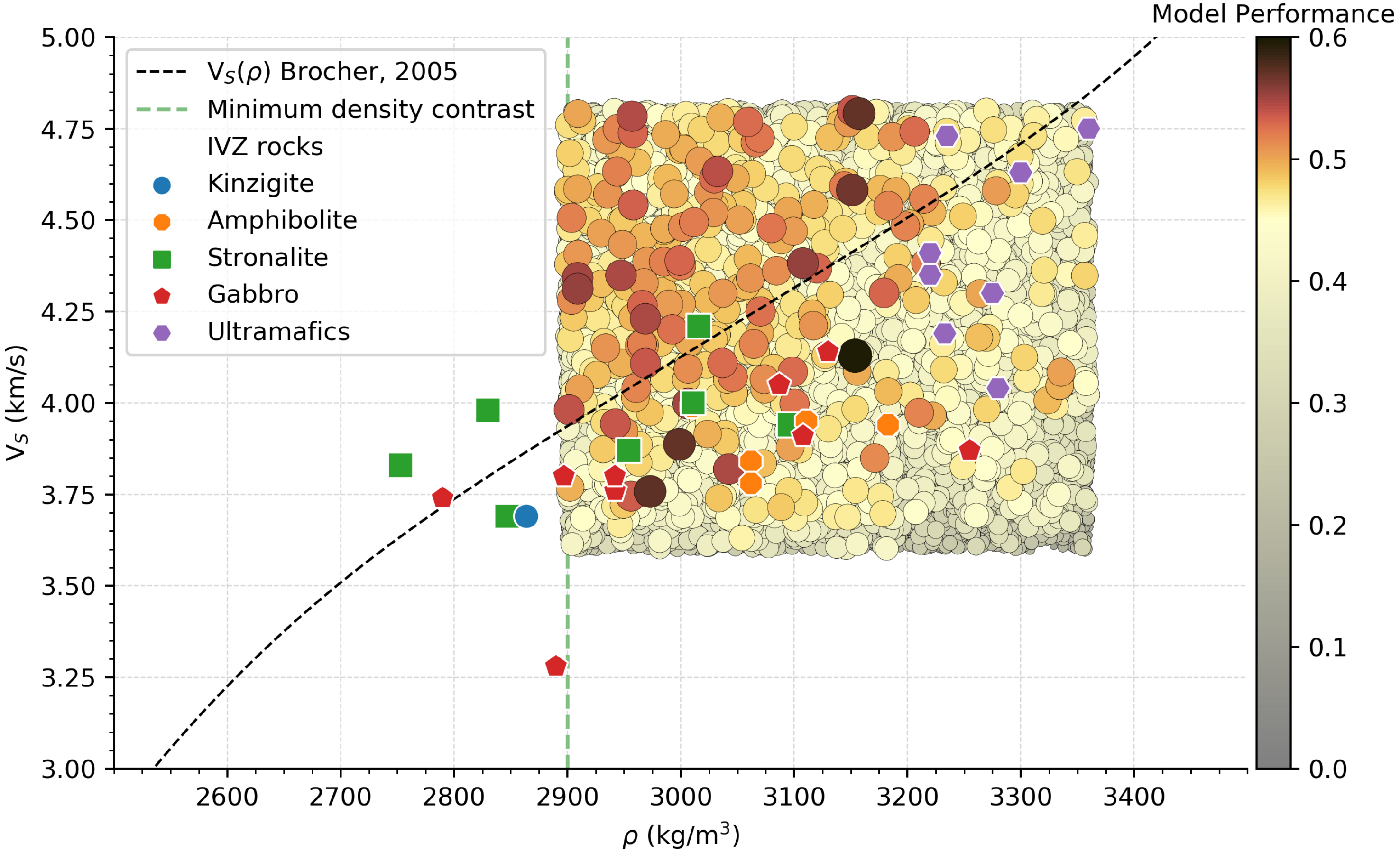

Inversion results on the density and shear-wave velocity contrasts associated with the 2D model interface, shown as gray-contoured circles of size and colour according to to the model performance. The background density and the background shear-wave velocity absolute values are common for all models (2700 kg/m^3 and 3.5 km/s respectively). For comparison, the regression fit for the vs(ρ) relationship from rocks discussed in Brocher (2005) (black dashed line) is shown together with a relevant set of rock physical properties across the IVZ from the SAPHYR catalog Zappone et al., (2015)

Interface sharpness investigation by frequency-dependent analysis (station IA02A)

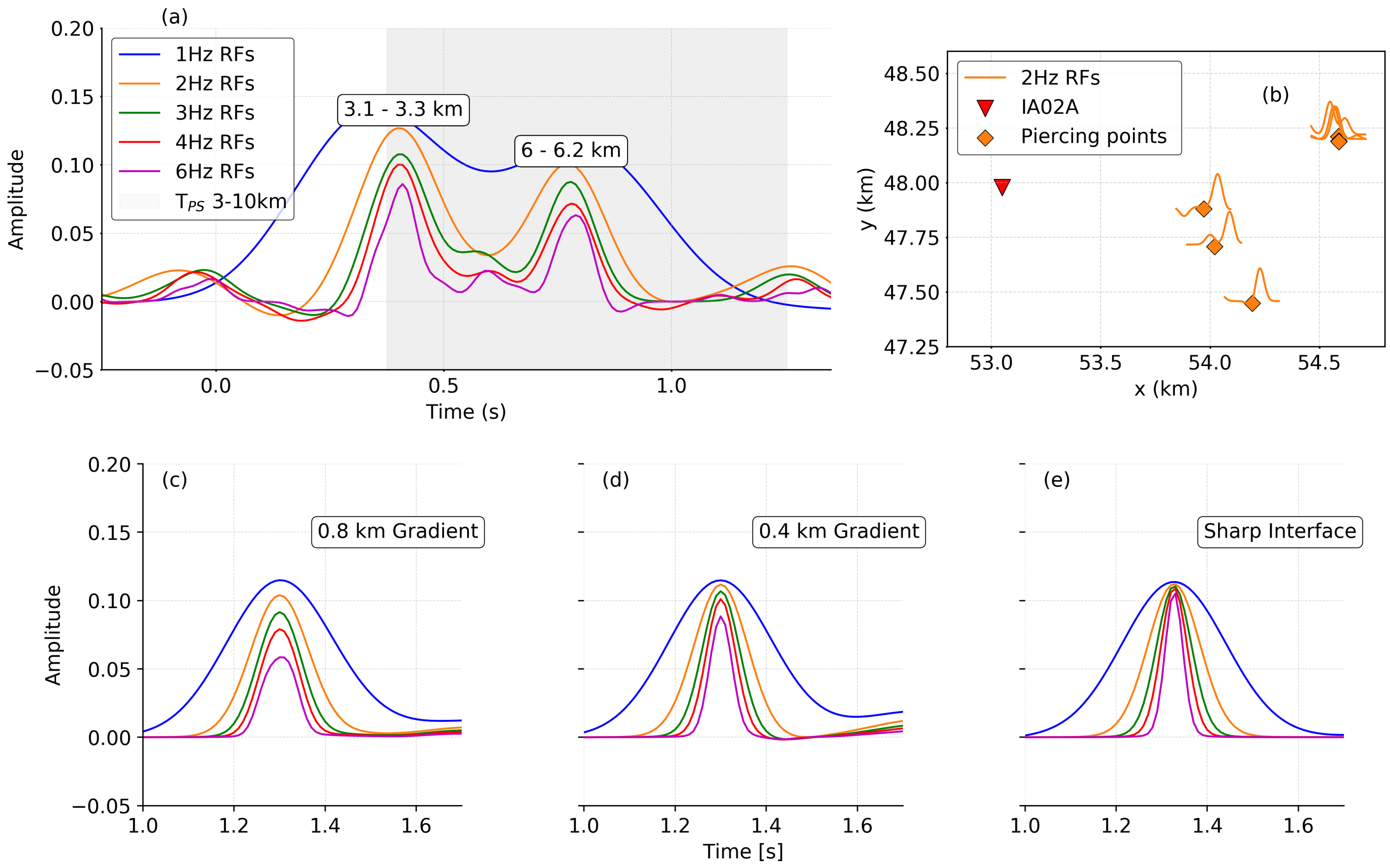

(a) Observed RFs stacked at different frequency ranges, from 0.1Hz to five different maximum frequencies as specified in the legend. The decreasing signal width, with increasing frequency, points towards a discontinuity sharper than the resolution of the highest frequency waves. The gray band in the background indicates the expected time delay for a P-to-S converted phase from a discontinuity located between 3 and 10 km depth, and with vs = 3.5 km/s above it. The estimated depth of the conversion for the two observed peaks is indicated

(b) Piercing point map (orange squares) for the traces that have been considered in panel (a), for the frequency range 0.1Hz to 2Hz. Next to each piercing point, the time interval 0 to 1s of the associated RFs is plotted, to highlight the spatial variability of the stacked RFs signals. (c-e) Synthetic RFs for the same frequencies as in (a) demonstrating the effect of velocity gradient sharpness on peak widths and amplitudes.

UNIL | Université de Lausanne
Institut des sciences de la Terre

Thank you very much for your attention!

For any discussion or comment, please use the EGU chat or feel free to contact matteo.scarponi@unil.ch

Acknowledgements

We are grateful to P. Jedlička and J. Kotek from Institute of Geophysics, Czech Academy of Sciences, for installation of their seismic stations within this project (stations of MOBNET pool granted by project CzechGeo/EPOS No. LM2015079 of the MEYS), to T. Berthet, L. Colavitti, S.Subedi, G. Moradi and C. Alvizuri for the discussions and fieldwork efforts, to Prof. P. Manzotti for scientific discussion, to Dr. T. Diehl for making the 3-D P-wave velocity model of the Alps available. This research is supported by the Swiss National Science Foundation grant number PP00P2_157627 and by the Grant Agency of the Czech Republic No. 21-25710.

References

- Scarponi, M., Hetényi, G., Berthet, T., Baron, L., Manzotti, P., Petri, B., Pistone, M., and Müntener, O., 2020, New gravity data and 3-D density model constraints on the Ivrea Geophysical Body (Western Alps): Geophysical Journal International, v. 222, no. 3, p. 1977-1991.

- Schmid, S. M., Fügenschuh, B., Kissling, E., and Schuster, R., 2004, Tectonic map and overall architecture of the Alpine orogen: Eclogae Geologicae Helvetiae, v. 97, no. 1, p. 93-117.

- Spada, M., Bianchi, I., Kissling, E., Agostinetti, N. P., and Wiemer, S., 2013, Combining controlled-source seismology and receiver function information to derive 3-D Moho topography for Italy: Geophysical Journal International, v. 194, no. 2, p. 1050-1068.

- Petri, B., Duretz, T., Mohn, G., Schmalholz, S. M., Karner, G. D., and Müntener, O., 2019, Thinning mechanisms of heterogeneous continental lithosphere: Earth and Planetary Science Letters, v. 512, p. 147-162.

- Zappone, A., Wenning, Q. C., and Kissling, E., SAPHYR: The Swiss Atlas of physical properties of rocks, in Proceedings 2015 AGU Fall Meeting2015, AGU.